PHYSICAL REVIEW B **78**, 201402(R) (2008)

High-energy optical conductivity of graphene determined by reflection contrast spectroscopy

Zhe Fei, Yi Shi, Lin Pu, Feng Gao, Yu Liu, L. Sheng, Baigeng Wang, Rong Zhang, and Youdou Zheng
Department of Physics and National Laboratory of Solid State Microstructure, Nanjing University, Nanjing 210093, China
(Received 8 October 2008; published 4 November 2008)

Optical conductivity $G(\omega)$ of graphene, which is famous for its universality close to the Dirac point, is determined from the visible to near-ultraviolet region by using reflection contrast spectroscopy. We find that the universality does not survive beyond the visible region. Instead, $G(\omega)$ increases rapidly with the energy, which is originated from the flat dispersion relation at the M point corresponding to an extraordinarily large density of states (DOS). The first-principles-calculated band structure and DOS spectrum explain well the high-energy behaviors of $G(\omega)$. Our work presents a more comprehensive map of graphene's optical conductivity and electronic structure.

DOI: 10.1103/PhysRevB.78.201402 PACS number(s): 81.05.Uw, 72.30.+q, 73.23.−b, 78.67.−n

The optical conductivity $G(\omega)$ of graphene[1,2] provides us the most intuitive understanding about the band-structure properties. It is predicted that there is a universal optical conductivity $G_0=e^2/4\hbar$ for monolayer graphene (MG), which is frequency independent and determined solely by the fundamental constants (e is the electron charge and $\hbar$ is the Planck constant divided by 2π).[3,4] This prediction is made based on the linear dispersion relation that provides equal optical interband transition probabilities among different photon energies. Nevertheless, the linear dispersion relation of graphene is valid only close to the Dirac point, where valence and conduction conical bands meet each other. As the energy increases and deviates from the Dirac point, the linear approximation fails gradually, which then affects the universality of the optical conductivity. Evidently, it is important to explore experimentally the behavior of $G(\omega)$ beyond the well-studied Dirac cone region. So far, direct experimental works concerning the optical conductivity of graphene are very few in number. Only recently, two graphene groups managed to obtain $G(\omega)$ in the visible and infrared regions, respectively, and verify the universality experimentally.[5,6] Herein, by extending the energy to the near-ultraviolet region, we directly determine the high-energy optical conductivity of graphene beyond the Dirac cone region through reflection contrast spectroscopy.

Reflection contrast spectroscopy has been proven to be an effective and convenient method for studying graphene.[7,8] In principle, it is actually a quantitative and analytical version of our eye observation, which is based sensitively on the contrast $1-R_{\text{sample}}/R_{\text{substrate}}$. R_{sample} and $R_{\text{substrate}}$ are reflectances of the graphene sample system and the substrate, respectively. Further explorations in this work show that the contrast is a combined effect of light absorption and reflection of bare graphene, which both depend directly on the optical conductivity. Using Maxwell's equations and boundary conditions, the light reflectance (R_g) and transmittance (T_g) of bare graphene can be deduced as follows with an assumption of the normal light incidence and ideal two-dimensional limit:[9]

$$T_g=|1+\alpha|^{-2}, \quad R_g=|1+\alpha^{-1}|^{-2}, \tag{1}$$

where $\alpha=c\mu_0 G/2$ is 188.4 times the optical conductivity; c and μ_0 are the light speed and magnetic permeability in a vacuum, respectively.

In this Rapid Communication, reflection contrast spectra of graphene were measured in the photon energies ranging from 1.54 to 4.13 eV. Based on Eq. (1) and the calculations concerning sample structural configuration, $G(\omega)$ was extracted from the measured spectra. With the wide energy scale, we observed not only the universality of $G(\omega)$ close to the theoretical expectations in the visible region, but also a rapid increase leaving the universal values in the near-ultraviolet region. The first-principles calculations of band structure and density of states (DOS) were employed to analyze the behaviors of $G(\omega)$.

Figure 1(a) gives the schematic diagram of our experiment's configuration, where a graphene sample lies on a SiO_2/Si substrate. The sample shown in Fig. 1(b) consists of two parts, where it is easy to identify the substrate, the MG, and the BG by the contrast differences among them. In addition to optical microscopy, Raman spectroscopy was also used to guarantee the quality of the graphene samples [Fig. 1(c)]. Here, the measurements of the reflection contrast spectra were performed by using a UV–visible–near-infrared (NIR) microspectrophotometer (CRAIC QDI 2010™). The focused light plotted in Fig. 1(a) is almost normal to the sample surface, with incident angles ranging from 0° to less than 11°. Calculation shows that the normal-incidence approximation only causes an error less than 1% in the present experimental situation. By adjusting the optical aperture, the incident light was focused to 6 μm, which is smaller than the graphene dimension. This microscopy makes it possible that all measured signals were collected under the same conditions. The measurements were carried out at room temperature.

Figure 2 presents the measured reflection contrast spectra of the samples, including MG, BG, and three thick graphite flakes. From the obvious differences among the measured curves shown in Fig. 2(a), one can see that reflection contrast spectroscopy is truly an effective way to identify graphite with different thicknesses.[7] For clarity, the zoomed-in curves for the MG and BG are replotted in Fig. 2(b). Two contrast peaks are clearly observed, which reminds one of the optimum light wavelengths used to detect graphene. Note that the distribution of the peaks depends mainly on the thickness of SiO_2; therefore the thickness has to be chosen carefully for different detection purposes. The reason for the 300-nm-thick SiO_2 being one of the most popular choices is that one

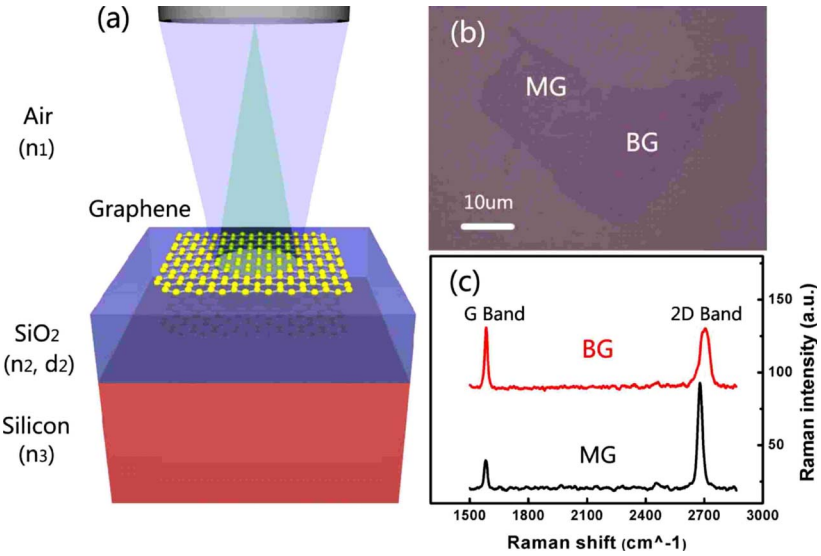

FIG. 1. (Color online) (a) Schematic diagram of our reflection contrast measurement. (b) Microscopic image of the graphene sample with MG and bilayer graphene (BG). The substrate is 380 μm n^+-doped ⟨110⟩-oriented silicon with 300 ± 10 nm dry thermal oxide on the top. (c) The Raman spectra of our sample. G band and $2D$ band are clearly observed, which are two characteristic signals used to identify graphene with different thicknesses (Ref. 10).

contrast peak (595 nm) is just at the center of the visible region and the total visible contrast approaches a maximum [Fig. 2(b)].

The whole optical transfer process can be expressed mathematically by the transmission-matrix formalism.[11] The complete transfer matrices of the bare substrate and the whole sample system can be given as follows:

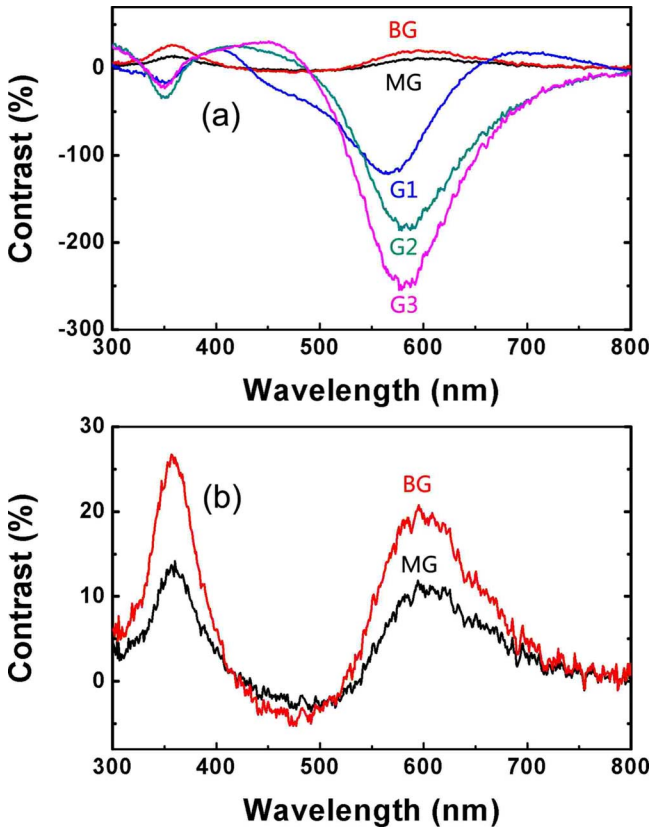

FIG. 2. (Color online) (a) 300–800 nm reflection contrast spectra for all samples including MG, BG, and three thick graphite layers G1, G2, and G3. Thickness of graphite: G3 > G2 > G1. (b) The zoomed-in reflection contrast spectra for the MG and BG.

$$M_{\text{substrate}} = M_{\text{Si}} M_{\text{ox}} M_e, \quad M_{\text{sample}} = M_{\text{Si}} M_{\text{ox}} M_g M_e, \tag{2}$$

where M_g, M_{Si}, and M_{ox} describe the optical transfer properties of the graphene, silicon substrate, and silicon dioxide layer, respectively. M_e represents the complex environmental influence, such as surface absorption of water, which is inevitable for a graphene sample in air atmosphere.[12] Based on Eq. (1), M_g can be written as follows:

$$M_g = \begin{bmatrix} 1-\alpha & -\alpha \\ \alpha & 1+\alpha \end{bmatrix}. \tag{3}$$

For simplicity, we first consider the ideal circumstance to suppose $M_e = I$ (I is the unit matrix). Accordingly, the reflectances of the bare substrate and whole sample system can be deduced on the basis of Eqs. (2) and (3) and Fresnel's equations. For a normal light incidence,

$$R_{\text{substrate}} = |r_{\text{substrate}}|^2 = \left| \frac{r_{32} e^{ik_2 d_2} + r_{21} e^{-ik_2 d_2}}{r_{32} r_{21} e^{ik_2 d_2} + e^{-ik_2 d_2}} \right|^2, \tag{4}$$

$$R_{\text{sample}} = \left| \frac{r_{\text{substrate}}(1-\alpha) + \alpha}{r_{\text{substrate}}(-\alpha) + (1+\alpha)} \right|^2, \tag{5}$$

where $r_{32} = n_2 - n_3 / n_2 + n_3$ and $r_{21} = n_1 - n_2 / n_1 + n_2$ are the relative indices of refraction. $r_{\text{substrate}}$ is the ratio between the electric components of the incident and reflected light of the substrate. n_1, n_2, and n_3 are the refractive indices [Fig. 1(a)]. We take $n_1 = 1$ for air and $n_2 = 1.47$ for SiO_2. n_3 is presented by LUXPOP.[13] d_2 is the thickness of SiO_2, and $k_2 d_2 = n_2 \omega d_2 / c$ is the light phase shift through the oxide layer. Based on Eqs. (4) and (5), the mathematical relation between $G(\omega)$ and the contrast is established. Consequently, $G(\omega)$ is obtained directly from the reflection contrast spectra of graphene. Here, we assume that the imaginary part of $G(\omega)$ equals zero in the present energy scale.[4,6,14,15] The parameters chosen for the substrate in the calculations are the main sources of error.

The obtained optical conductivity is given in Fig. 3(a). It spreads in two energy regions: region A (1.6–2.2 eV) is in the visible region, while region B (3.0–3.8 eV) is almost in

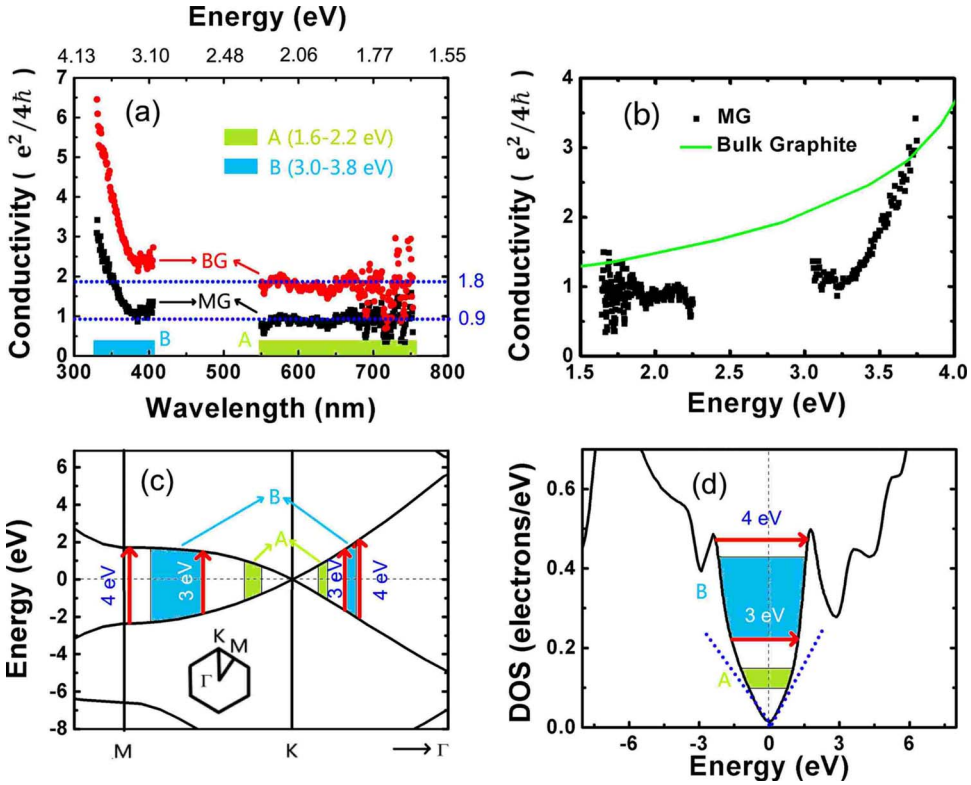

FIG. 3. (Color online) (a) Experimentally obtained $G(\omega)$ in the energy regions A and B. (b) Comparison between optical conductivity of MG and sheet conductance of bulk graphite. (c) First-principles calculation of MG's band structure close to the K point. (d) First-principles calculation of MG's DOS spectrum. Blue dashed lines in (d) represent the linear relation between DOS and energy close to the Dirac point. Red arrows plotted in (b) and (c) represent the photon-induced electron transitions with energies of 3 and 4 eV. The colored regions in (b) and (c) cover the electron transition positions with photon energies in regions A and B.

the near-ultraviolet region. Notably, $G(\omega)$ behaves differently in the two regions. In region A, $G(\omega)$ is nearly constant with $G_{\mathrm{MG}}=0.9e^2/4\hbar$ for the MG and $G_{\mathrm{BG}}=1.8e^2/4\hbar$ for the BG, which are systematically lower than the theoretical expectations G_0 and $2G_0$. This is an inevitable result of the ideal-circumstance approximation, $M_e=I$, which will be discussed below. In region B, nevertheless, $G(\omega)$ increases rapidly with the photon energy. Within a narrow energy region of 3.0–3.8 eV, the remarkable increase in $G(\omega)$ is up to three times, which is from $1.2e^2/4\hbar$ to $3.3e^2/4\hbar$ and $2.4e^2/4\hbar$ to $6.6e^2/4\hbar$ for the MG and BG, respectively. Unlike in regions A and B, $G(\omega)$ could not be given accurately in the other regions under the present sample parameters, where the contrasts of graphene are close to zero [Fig. 2(b)]. By modulating the thickness of SiO_2 experimentally, $G(\omega)$ in these blind energy regions would be obtained. In Fig. 3(b), we make a comparison between $G(\omega)$ of the MG and optical sheet conductance of bulk graphite, which is converted from the optical data in previous works.[16,17] The rapid increase can also be seen in bulk graphite. Yet the dimensional difference is still obvious in the present energy scale, which reveals that the electronic structure of graphene is modified from the one of bulk graphite.

The behaviors of $G(\omega)$ shown in Fig. 3(a) are just the exterior performances of the special electronic structure of graphene. Figures 3(c) and 3(d) plot the curves obtained from the first-principles calculations of MG's band structure and DOS, which are in agreement with the previous works.[18,19] The Dirac fermion picture for graphene ($E=\hbar k v_F$) is valid only close to the Dirac point. v_F is the Fermi velocity of graphene. Here, the DOS $D(\omega)=(dN/dk)/(dE/dk)\propto k/v_F=\omega/v_F^2$ has a linear relation with energy. Therefore, the optical conductivity $G(\omega)\propto D(\omega/2)/\omega$ tends to be a universal constant G_0 independent of frequency.[14] As the photon energy increases up to the visible region around 2 eV, the triangular warping and nonlinear effects appear and result in a slight deviation of DOS from the normal linear value [region A in Figs. 3(c) and 3(d)]. The increase in DOS is very limited in the visible region. Consequently, the universality of $G(\omega)$ still exists approximately as has been verified by the experimental observation [region A in Fig. 3(a)].

As the photon energy further increases up to the near-ultraviolet region, the universality of $G(\omega)$ totally disappears. Note that both the valence and conduction bands turn flat near the M point, where the photon transition energy is close to 4 eV [Fig. 3(c)]. The reason why the optical conductivity increases with energy is that the flat dispersion relation corresponds to an extraordinarily large DOS, which leads to a greatly enhanced interband transition probability. Approximate estimation based on Fig. 3(d) shows that the $G(\omega)$ of MG is more than three times the universal value as the photon energy approaches 4 eV, agreeing well with our experimental data in region B. This rapid increase in $G(\omega)$ in the near-ultraviolet region was predicted by recent theoretical work.[14] Since the absorption coefficient of graphene, $P_g=1-T_g-R_g\simeq 2\alpha$, is proportional to $G(\omega)$, the opacity of graphene in 4 eV reaches the maximum more than three times that in the visible region, which makes much sense in detection of a suspended graphene.[10]

In order to understand well the origin of the contrast of graphene, furthermore, we present systematic analysis considering the optical transfer process. In general, the contrast is a combined effect of both the reflection and absorption of bare graphene. Based on the universal optical conductivity G_0 of MG in the visible region, one can calculate with Eq.

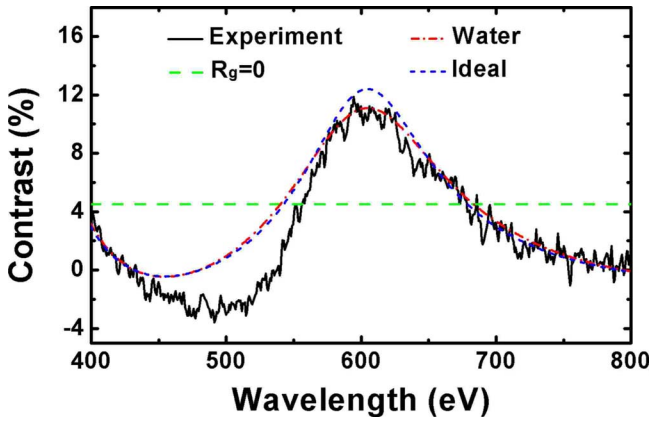

FIG. 4. (Color online) Comparison of calculated reflection contrast spectra of graphene with (red dot-dashed curve) and without (blue short-dashed curve) considering the surface absorption of water. The calculated result is almost unchanged among different thicknesses of water around 1 nm. The green dashed line is the calculated contrast spectrum under assumption of zero reflectance of graphene (R_g=0). The black curve is the experimental reflection contrast spectrum of MG.

(1) that the transmittance T_g, reflectance R_g, and absorption coefficient P_g are 97.7%, 0.013%, and 2.3%, respectively. Note that the 2.3% absorption of light by graphene makes much sense to the contrast. The light beam transmits through the graphene twice in the transfer process. Hence a constant 4.5% contrast spectrum is obtained only in consideration of the light absorption (green dashed line in Fig. 4). However, the actual contrast spectrum is an energy-dependent curve rather than a horizontal line, which can be attributed to the minor reflection of graphene. Although the reflectance by MG is only 0.013%, very close to zero, it contributes dramatically to the contrast due to the light interference. The discussions about BG can also be given accordingly.

Now we go back to consider the environmental influence resulting in $M_e \neq I$, which is typically surface absorption of water, which is inevitable in air atmosphere. Suppose the graphene sample and substrate are both covered by a film of water with a thickness d ($d \simeq 1$ nm under normal circumstances); the calculations are given in Fig. 4. One can see that surface absorption of water makes the contrast lower than that in an ideal circumstance, and consequently results in systematic deviation: $G_{\mathrm{MG}} < G_0$ and $G_{\mathrm{BG}} < 2G_0$ [Fig. 3(a)]. Therefore, by considering the surface absorption of water in the calculation of Eq. (2), the obtained optical conductivity is very close to the theoretical expectations.

In summary, we provide a comprehensive method for studying graphene and determining the optical conductivity with reflection contrast spectroscopy. It is found that $G(\omega)$ is nearly constant with the theoretical predicted values in the visible region. As the photon energy increases up to the near-ultraviolet region approaching 4 eV (the photon transition energy at the M point), $G(\omega)$ increases rapidly with the energy. We give the first-principles-calculated band structure and DOS spectrum of graphene, which explain well the high-energy behaviors of $G(\omega)$. Our work reveals more aspects of graphene's optical and electronic properties, and gives inspiration for more effective detection of graphene in the near-ultraviolet region.

This work was financially supported by the "973" Program under Grant No. 2007CB925100 and the NSFC under Grants No. 60676006 and No. 90606021. We thank Ruwen Peng from Nanjing University and Xiaolong Chen from Chinese Academy of Sciences for the experimental and theoretical support, respectively.

[1] A. K. Geim and K. S. Novoselov, Nature Mater. **6**, 183 (2007).
[2] K. S. Novoselov, A. K. Geim, S. V. Dubonos, E. W. Hill, and I. V. Grigorieva, Nature (London) **438**, 197 (2005).
[3] V. P. Gusynin and S. G. Sharapov, Phys. Rev. Lett. **95**, 146801 (2005).
[4] L. A. Falkovsky and A. A. Varlamov, Eur. Phys. J. B **56**, 281 (2007).
[5] R. R. Nair, P. Blake, A. N. Grigorenko, K. S. Novoselov, T. J. Booth, T. Stauber, N. M. R. Peres, and A. K. Geim, Science **320**, 1308 (2008).
[6] Z. Q. Li, E. A. Henriksen, Z. Jiang, Z. Hao, M. C. Martin, P. Kim, H. L. Stormer, and D. N. Basov, Nat. Phys. **4**, 532 (2008).
[7] Z. H. Ni, H. M. Wang, J. Kasim, H. M. Fan, T. Yu, Y. H. Wu, Y. P. Feng, and Z. X. Shen, Nano Lett. **7**, 2758 (2007).
[8] F. Wang, Y. Zhang, C. Tian, C. Girit, A. Zettl, M. Crommie, and Y. R. Shen, Science **320**, 206 (2008).
[9] A. B. Kuzmenko, E. van Heumen, F. Carbone, and D. van der Marel, Phys. Rev. Lett. **100**, 117401 (2008).
[10] I. Calizo, A. A. Balandin, W. Bao, F. Miao, and C. N. Lau, Nano Lett. **7**, 2645 (2007).
[11] S. Roddaro, P. Pingue, V. Piazza, V. Pellegrini, and F. Beltram, Nano Lett. **7**, 2707 (2007).
[12] J. Sabio, C. Seoanez, S. Fratini, F. Guinea, A. H. Castro Neto, and F. Sols, Phys. Rev. B **77**, 195409 (2008).
[13] LUXPOP, thin film and bulk index of refraction and photonics calculations; website: www.luxpop.com.
[14] T. Stauber, N. M. R. Peres, and A. K. Geim, Phys. Rev. B **78**, 085432 (2008).
[15] The imaginary part can probably be induced by nonideal effects (e.g., the substrate); therefore we perform calculations to evaluate the influence. Results show that the influence is very limited, even when the imaginary part reaches a measurable quantity (e.g., $0.4G_0$).
[16] E. A. Taft and H. R. Philpp, Phys. Rev. **138**, A197 (1965).
[17] A. B. Djurisic and E. H. Li, J. Appl. Phys. **85**, 7404 (1999).
[18] S. Latil and L. Henrard, Phys. Rev. Lett. **97**, 036803 (2006).
[19] E. J. Duplock, M. Scheffler, and P. J. D. Lindan, Phys. Rev. Lett. **92**, 225502 (2004).